Progress In Electromagnetics Research C, Vol. 85, 105–116, 2018

Gain Enhancement of a Millimeter Wave Antipodal Vivaldi Antenna by Epsilon-Near-Zero Metamaterial

Shaza El-Nady[1, *], Hany M. Zamel[1], Moataza Hendy[1], Abdel H. A. Zekry[2], and Ahmed M. Attiya[1]

Abstract—In this paper a compact antipodal Vivaldi antenna with dimensions of $40 \times 85\,\text{mm}^2$ for Ka band is presented. To enhance the antenna gain epsilon near zero metamaterial (ENZ) unit cells are embedded at the same plane of the Vivaldi flare aperture. These ENZ unit cells have the advantage of confining the radiated fields with additional compact size. The obtained antenna exhibits an ultra-wide bandwidth from 23 GHz to 40 GHz with a reflection coefficient less than -10 dB. This is suitable for 5G applications at both 28 and 38 GHz. The antenna gain in this frequency band is found in the range from 14 to 17.2 dBi. The proposed antenna is designed by using CST-MW Studio, and the results are verified with experimental measurements.

1. INTRODUCTION

Studying the properties of metamaterials attracts significant interest due to their special electromagnetic characteristics which cannot be found in natural materials. These unique characteristics include double negative (DNG) refractive index metamaterials [1, 2], epsilon near zero (ENZ) metamaterials [3–5], and mu near zero metamaterials (MEZ) [6]. These metamaterials can be synthesized by embedding suitable inclusions in periodic forms inside a hosting medium [7].

In ENZ metamaterials the phase velocity of propagating electromagnetic waves tends to infinity. Thus, the resulting wave length also tends to infinity. In this case the phases of the fields at the two ends of an arbitrary shaped slab of an ENZ metamaterial are nearly the same. This property has a great importance in antennas. Conventional antennas like dipole antenna have a wide beamwidth radiation pattern with a spherical wave front. An ENZ slab with an appropriate shape can be used to convert these spherical wave fronts to nearly planar wave fronts. Thus, the resulting radiation pattern would have a confined pattern with high directivity [8]. ENZ metamaterials are shown to have interesting applications, such as increasing transmission through a subwavelength narrow aperture [9], increasing the directivity of antenna [10, 11], and tailoring the radiation pattern of radiators [12]. Scattering and propagation in the presence of ENZ metamaterials are studied in [13]. Based on this study, it is found that according to Snell's law, the refracted rays from an arbitrary radiating source embedded inside an ENZ metamaterial would introduce normal rays on the interface between the ENZ medium and free space. This property is quite useful in tailoring the wave front and controlling the direction of radiation for any antenna [14, 15].

On the other hand, millimeter-wave wide band antennas with a compact size and high gain are required for many applications such as mm-wave radars, high resolution imaging system and (5G) communication system [16–18]. Antipodal Vivaldi antenna (AVA) is a good candidate for millimeter-wave applications because it has a simple structure, light weight, compact size, high performance, ultra-wide bandwidth and nearly symmetric beam in E and H planes [19, 20]. Even with the advantages of

Received 3 May 2018, Accepted 25 June 2018, Scheduled 9 July 2018

* Corresponding author: Shaza El-Nady (shazaelnady@yahoo.com).

[1] Electronics Research Institute, Cairo, Egypt. [2] Faculty of Engineering, Ain Shams University, Egypt.

the Vivaldi antenna, it has some weak points such as tilted beam low directivity and low gain [21, 22]. Different techniques can be used to overcome these disadvantages such as using an array of Vivaldi antennas. However, this solution increases the total size.

Other techniques are discussed for improving the properties of Vivaldi antenna. A technique is based on adding a metal director in the front of the flaring of the Vivaldi [23]. This technique is used to increase the antenna gain up to 14.6 dBi in the frequency band from 2 to 40 GHz. Another technique is based on adding a trapezoidal dielectric slab in the front of the flaring as discussed in [24]. This technique could be used to obtain antenna gain of only 14 dBi.

In this paper, we incorporate the features of ENZ metamaterials and conventional Vivaldi antenna together to improve the characteristics of an original Vivaldi antenna. The required antenna gain in the present case is more than 16 dBi. The present antenna is proposed to be used in Ka band in the frequency range from 23 to 40 GHz. This is quite suitable for 5G applications at both 28 and 38 GHz. The proposed ENZ metamaterial is composed of periodic cells with a modified H-shape. These cells are embedded as a director in the front of the Vivaldi antenna to reduce the effective permittivity in endfire direction of the antenna.

The analysis of the proposed ENZ metamaterial is presented in Section 2. In Section 3, the detailed design of Vivaldi antenna is presented, and the effect of adding ENZ cells on the proposed antenna is studied. In Section 4, the experimental verifications of the designed Vivaldi antenna with ENZ cells are presented.

2. DESIGN OF ENZ METAMATERIAL

In this section, the design of the proposed ENZ metamaterial is discussed. The ENZ metamaterial in the present case is composed of periodic patches printed on a dielectric slab with a periodicity which is much smaller than the operating wavelength. By controlling the shape of these patches and the spacing between them, it is possible to control the resulting equivalent dielectric permittivity. In the present case, the epsilon near zero has only one component of permittivity tensor close to zero. Fig. 1 shows the geometry of the proposed unit cell obtained from [25]. The dimensions of this unit cell are presented in Table 1. Two dimensions, a and b, are varied to tune this unit cell for the required operating frequency range. These cells are periodic in the x-direction, and the proposed epsilon near zero is obtained in the y-direction [26]. This unit cell corresponds to an equivalent LC circuit. The quasi mender line in the x-direction corresponds to the inductive part while the parallel y-arms corresponds to the capacitive effect between the adjacent cells. The dimensions of the unit cell are optimized here to operate in the Ka frequency band. The substrate is assumed to be Rogers RO4003C with a dielectric constant $\varepsilon_r = 3.38$, loss tangent $\tan\delta = 0.0021$ and dielectric thickness $h = 0.2$ mm.

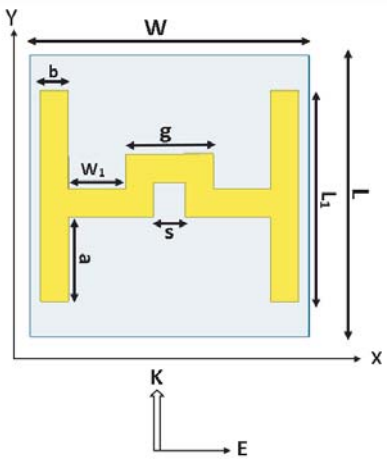

Figure 1. Geometry of the proposed unit cell of the ENZ metamaterial.

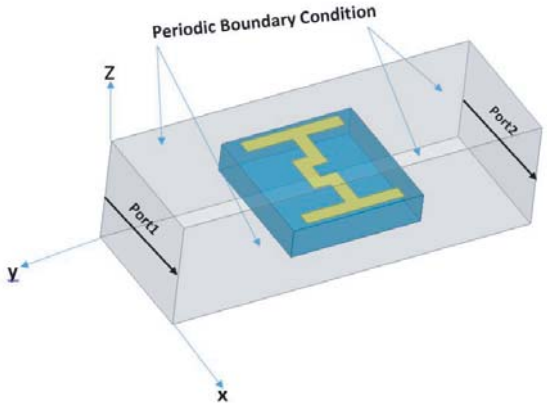

Figure 2. Simulation of electromagnetic wave propagation through a unit cell of ENZ metamaterial in periodic boundary conditions.

Table 1. Dimensions of the proposed unit cell.

L	W	L_1	W_1	g	S
2.27 mm	2.27 mm	1.7 mm	0.464 mm	0.716 mm	0.26 mm

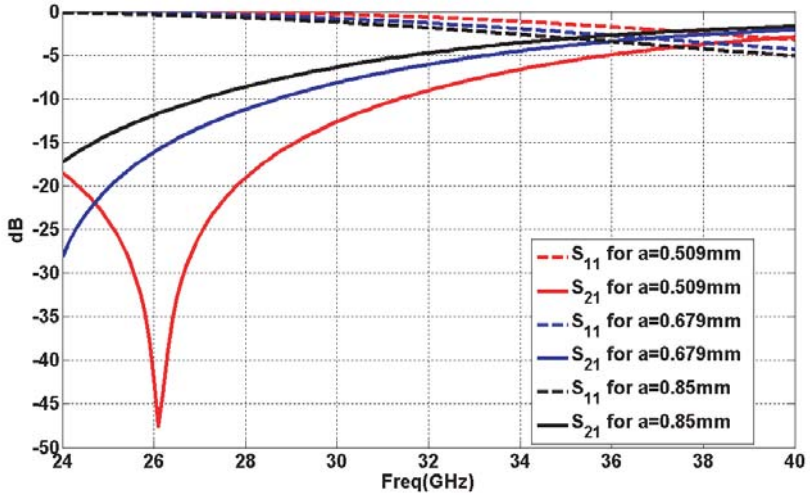

(a)

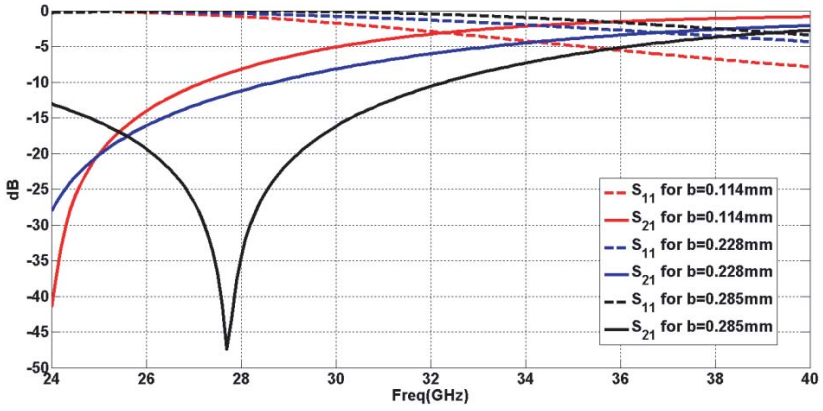

(b)

Figure 3. Reflection and transmission coefficients of a unit cell of ENZ metamaterial in periodic boundary conditions. (a) The dimension $b = 0.228$ mm and the dimension a is variable. (b) The dimension $a = 0.679$ mm and the dimension b is variable.

Reflection and transmission of electromagnetic waves through these periodic cells can be simulated by using a single cell inside periodic boundary conditions as shown in Fig. 2. Fig. 3 shows the obtained reflection and transmission coefficients for different dimensions of this unit cell. The dimensions a and b are varied to adjust the center frequency of the operating frequency range of the proposed ENZ metamaterial.

These reflection and transmission coefficients are used to retrieve the equivalent constitutive parameters as follows [27, 28]:

$$\varepsilon = \frac{n}{z} \tag{1a}$$

$$\mu = nz \tag{1b}$$

where

$$z = \pm\sqrt{\frac{(1+s_{11})^2 - s_{21}^2}{(1-s_{11})^2 - s_{21}^2}} \tag{1c}$$

and

$$n = \frac{1}{k_0 L}\left\{[\mathrm{Im}\left[\ln(A)\right] + 2m\pi] + j\mathrm{Re}\left[\ln(A)\right]\right\} \tag{1d}$$

where

$$A = \frac{s_{21}}{1 - s_{21}\frac{z-1}{z+1}} \tag{1e}$$

where s_{11} and s_{21} are reflection and transmission coefficients, respectively; k_0 is the free space propagation wave number; L is the length of the unit cell; m is an integer value related to the branch index of the refractive index n; z is the wave impedance; μ is the equivalent permeability; ε is the equivalent permittivity.

Figure 4 shows the obtained equivalent relative permittivity of this metamaterial for different values of a and b. It can be noted that the center frequency of the ENZ characteristics is decreased by increasing the dimension a as shown in Fig. 4(a). This can be explained due to the increase of the equivalent capacitance between the adjacent cells. On the other hand, increasing the dimension b decreases the equivalent inductance of the quasi mender line in the modified H-shape cell. Thus,

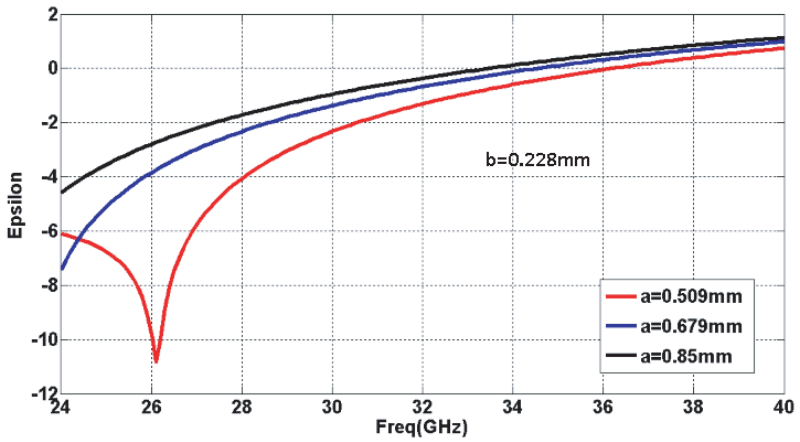

(a)

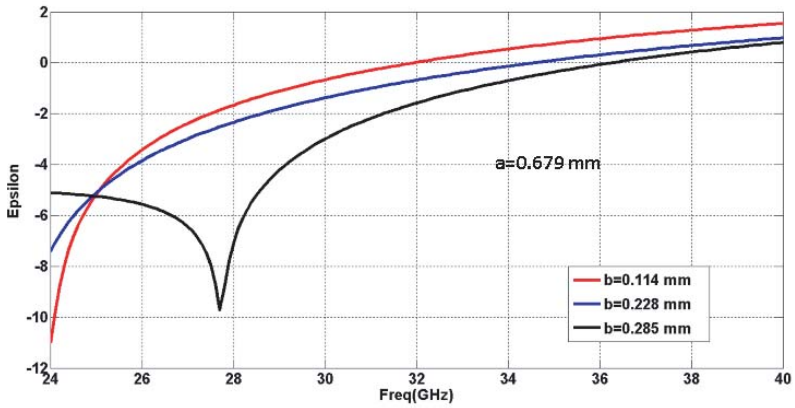

(b)

Figure 4. Equivalent relative dielectric constant in y-direction versus frequency with variation of a length a and (b) width b.

increasing the dimension b also increases the center frequency of the ENZ characteristics as shown in Fig. 4(b). Based on this parametric study, the optimum values of a and b for the required bandwidth are 0.679 mm and 0.228 mm, respectively.

3. GAIN ENHANCEMENT OF VIVALDI ANTENNA BASED ON EMBEDDING ENZ UNIT CELL

Vivaldi antenna is a traveling wave antenna, with a property of ultra-wide bandwidth, which operates as a resonant antenna at low frequencies and as a traveling wave radiator at high frequencies. The Vivaldi antenna is constructed of a pair of radiators, etched on the opposite sides of the dielectric substrate as shown in Fig. 5. The waves travel through the inner edges of the flared aperture then couple to each other to produce the radiation. The upper arm of the radiator is connected to a microstrip line while the lower arm is connected to partial ground plane. The Vivaldi antenna is fed through this microstrip

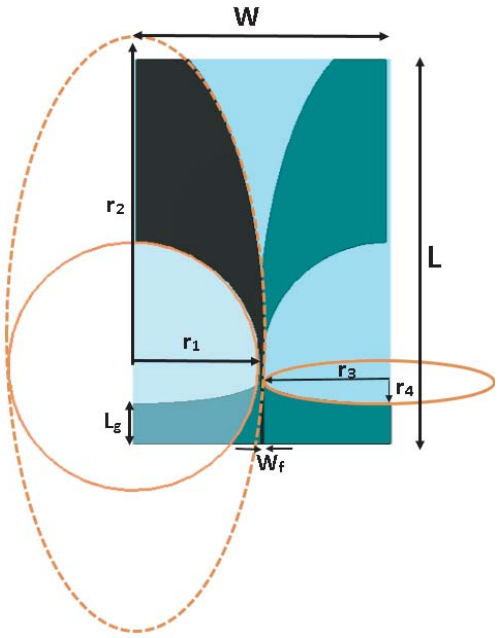

Figure 5. Geometry of a Vivaldi antenna.

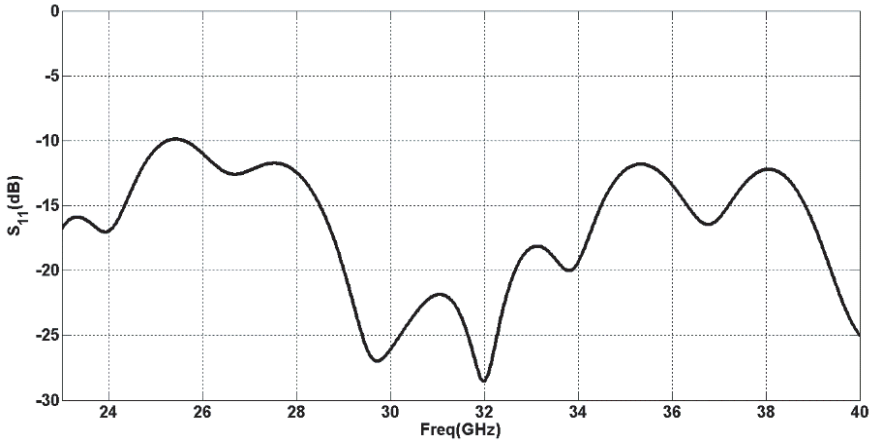

Figure 6. Reflection coefficient of the designed Vivaldi antenna.

Table 2. Dimensions of the proposed Vivaldi antenna.

L	W	L_g	W_f	r_1	r_2	r_3	r_4
60 mm	40 mm	6.19 mm	0.46 mm	19.405 mm	34.405 mm	19.67 mm	3.8 mm

line by using a coaxial connector. The dimensions of the proposed Vivaldi antenna are optimized to be operating in the frequency range from 23 to 40 GHz for 5G applications. The optimized dimensions of this antenna are presented at Table 2. Fig. 6 shows the reflection coefficient of the designed antenna at the required operating frequency band. It can be noted that the reflection coefficient is almost below −15 dB in all the required bands. Fig. 7 shows the antenna gain of this Vivaldi antenna. It can be noted that the obtained average antenna gain in the required band is slightly above 10 dBi.

To improve the characteristics of the designed Vivaldi antenna, an array of ENZ unit cells are added at its aperture. The ENZ unit cells are added on the axis of symmetry of the antenna aperture to concentrate the radiated fields in the endfire direction. Two configurations are studied here. The first configuration is based on increasing the substrate of the Vivaldi antenna with the same width

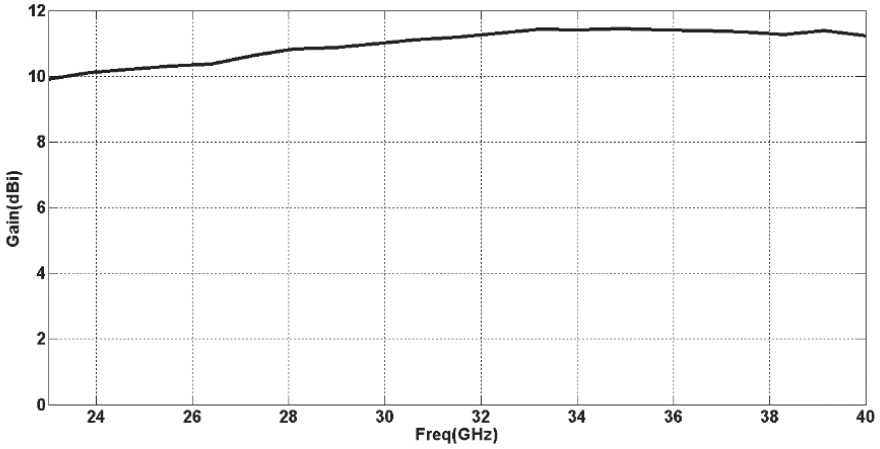

Figure 7. Antenna gain of the designed Vivaldi antenna.

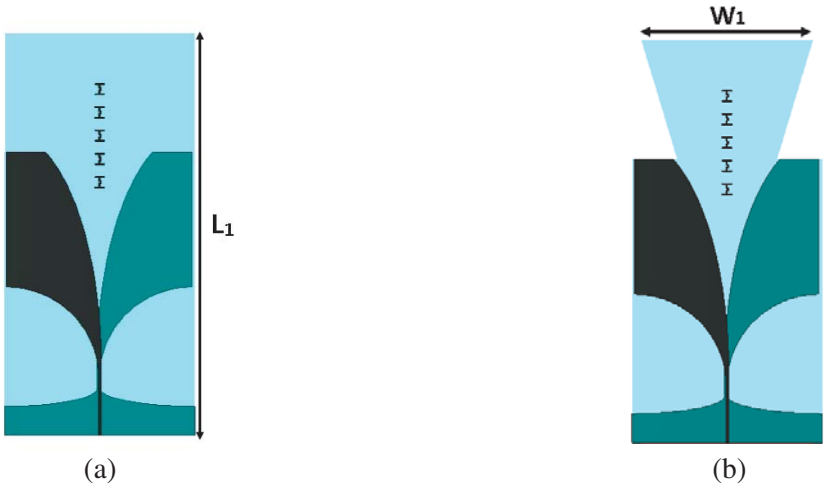

Figure 8. Modified Vivaldi antennas loaded with ENZ unit cell. (a) Configuration 1, $L_1 = 85$ m. (b) Configuration 2, $W1 = 36$ m.

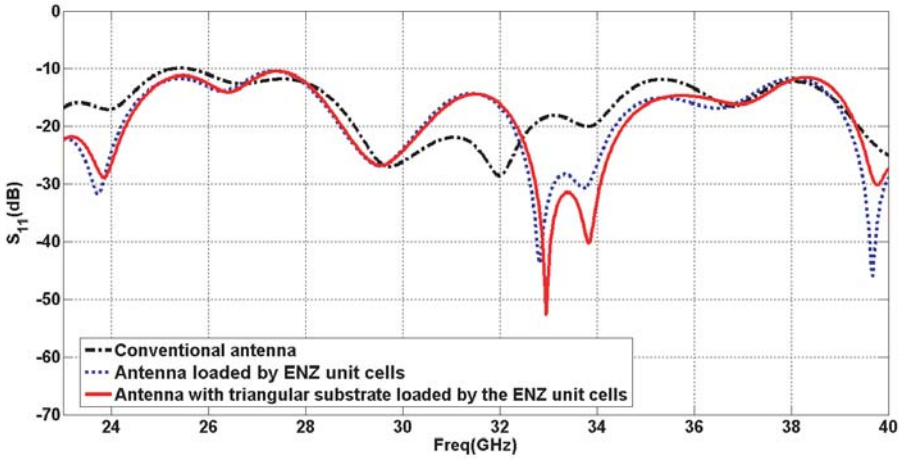

Figure 9. Comparison between the reflection coefficient of conventional Vivaldi antenna and the two modified configurations shown in Fig. 8.

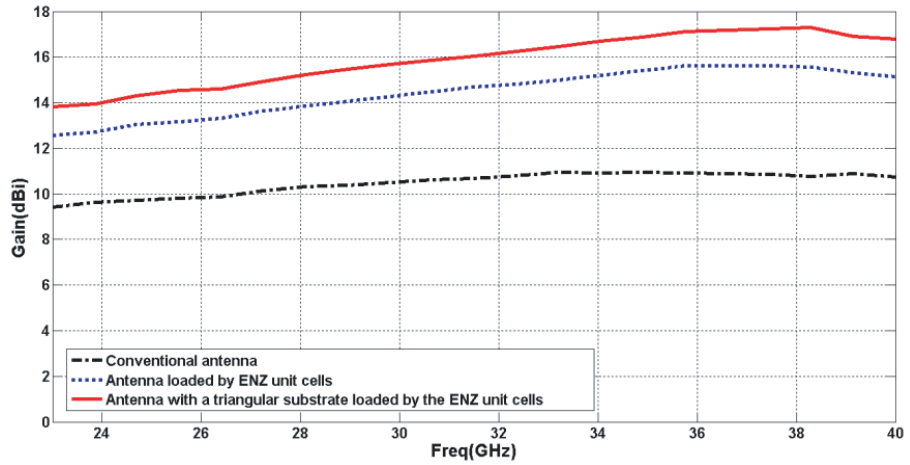

Figure 10. Comparison between the antenna gain of conventional Vivaldi antenna and the two modified configurations shown in Fig. 8.

of the original antenna and loading the extended part by unit cells of ENZ metamaterial as shown in Fig. 8(a). The second configuration is based on extending the flared aperture with a triangular substrate loaded by the ENZ unit cells as shown in Fig. 8(b). Fig. 9 shows a comparison between the reflection coefficients of the conventional Vivaldi antenna and the two modified configurations. It can be noted that the matching in the two modified configurations is improved in most of the operating band compared with the conventional Vivaldi antenna. In addition, Fig. 10 shows another comparison of the antenna gain for the three cases. It can be noted that adding ENZ unit cells improves the gain of the Vivaldi antenna. It can also be noted that the second configuration in Fig. 8(b) has a better gain than the first configuration by almost 2 dB. In this case the antenna gain is improved compared with the conventional Vivaldi antenna by nearly 5 dB over all the operating frequency band.

Figure 11 shows the radiation patterns of the three antennas in both E-plane (XY-plane) and H-plane (YZ-plane), at 28 and 38 GHz. It can be noted that adding ENZ unit cells reduces the beam width in both E and H planes.

Table 3 shows comparisons in terms of size, relative permittivity, and gain between the second modified configuration and other similar previously published antennas. It can be noted that the proposed antenna has some distinct advantages such as high gain and relatively compact size.

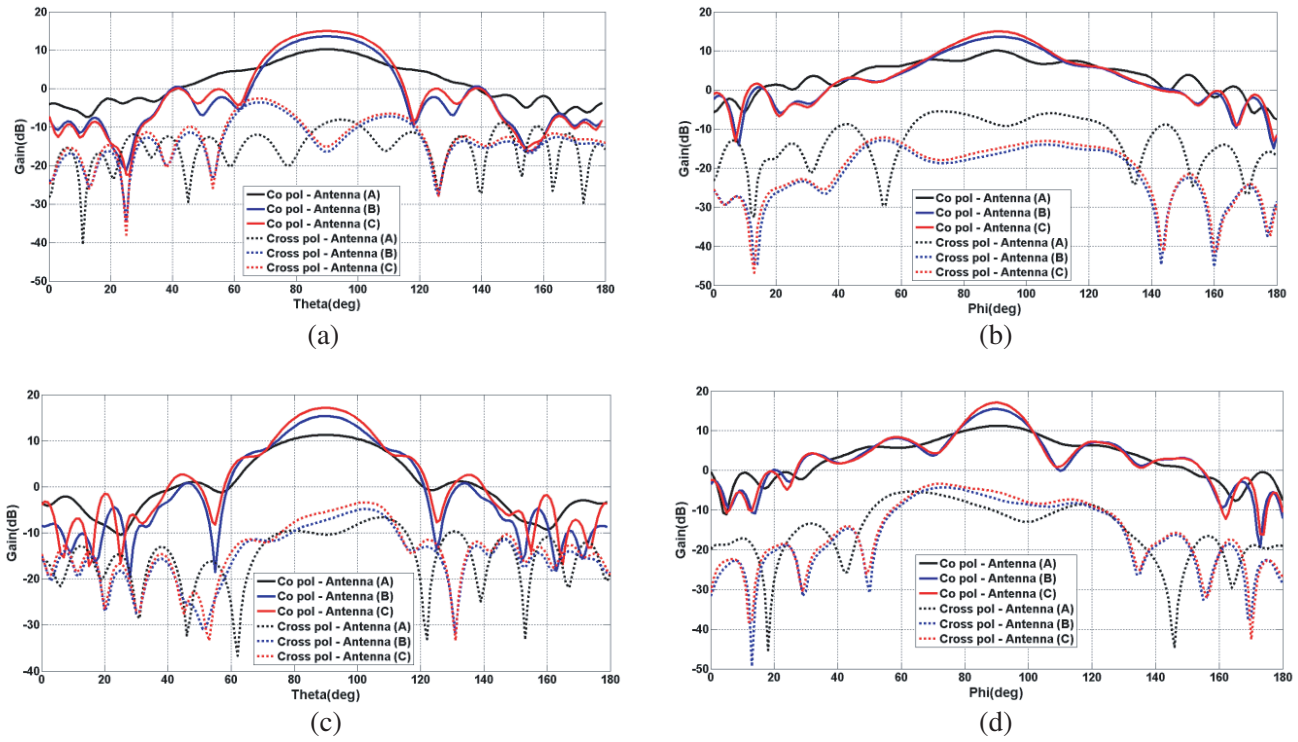

Figure 11. Comparisons between radiation pattern of conventional Vivaldi and the two modified configurations at different frequencies. (a) H-Plane @ 28 GHz. (b) E-Plane @ 28 GHz. (c) H-Plane @ 38 GHz. (d) E-Plane @ 38 GHz.

Table 3. Comparisons between the modified Vivaldi antenna and previously published work.

Ref.	Dimensions (mm^3)	Relative Permittivity	Freq. (GHz) → Gain (dBi)
[29]	$50 \times 66.4 \times 1$	4.5	30 GHz → 5 dBi
[30]	$66 \times 140 \times 1.5$	2.94	30 GHz → 5 dBi
[23]	$44 \times 98 \times 3$	2.2	40 GHz → 10.5 dBi
[31]	$40 \times 80 \times 0.508$	3.38	40 GHz → 9 dBi
[32]	$40 \times 90 \times 0.508$	3.38	40 GHz → 14.6 dB
[33]	$80 \times 24 \times 0.254$	2.2	40 GHz → 15.5 dBi
[34]	$57.5 \times 60.7 \times 0.508$	3.38	40 GHz → 13.8 dBi
This work	$40 \times 85 \times 0.2$	3.38	30 GHz → 15.7 dBi 40 GHz → 16.8 dBi

4. EXPERIMENTAL RESULTS

The fabricated modified Vivaldi antenna with an array of ENZ unit-cells is shown in Fig. 12. Both proposed antenna and unit cells are constructed on a Rogers RO4003C dielectric substrate. A 1.85 mm end-launch Southwest connector was used in the measurement of the antenna characteristics. The measured reflection coefficient of the proposed Vivaldi antenna is shown in Fig. 13. The measurements were performed by using ZVA 67 vector network analyzer. Good agreement between the measured and simulated reflection coefficients is obtained as shown in Fig. 13. Fig. 14 shows the experimental setup for measuring the peak antenna gain by using two identical antennas [35]. The comparison between

Figure 12. Fabricated modified Vivaldi antenna loaded by ENZ unit cells.

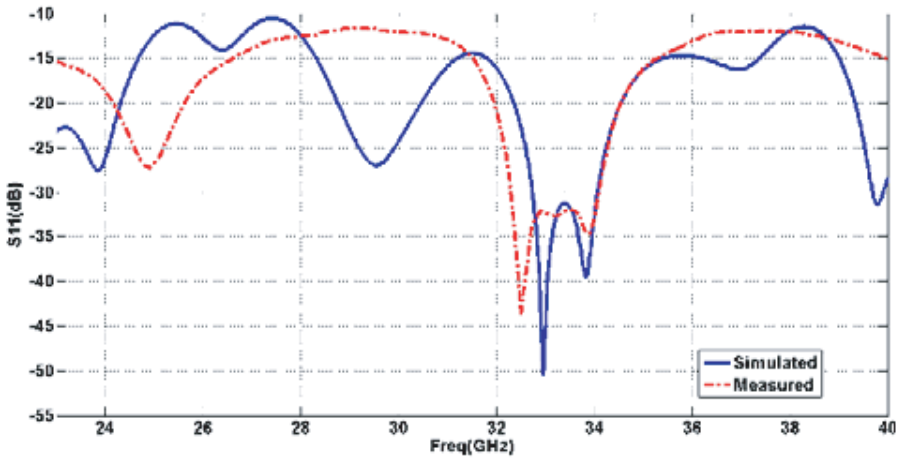

Figure 13. Comparison between the measured and simulated reflection coefficient of the modified Vivaldi antenna.

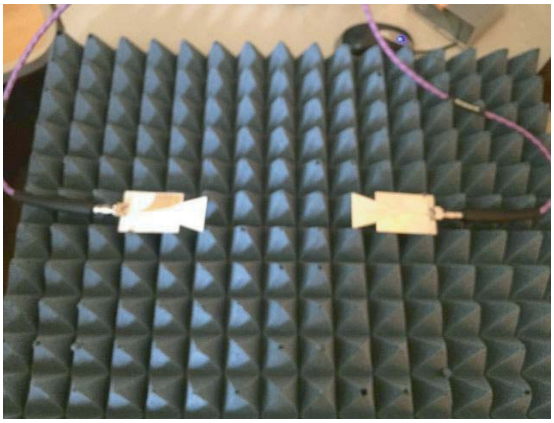

Figure 14. Measurement setup for antenna gain by two-identical antenna method.

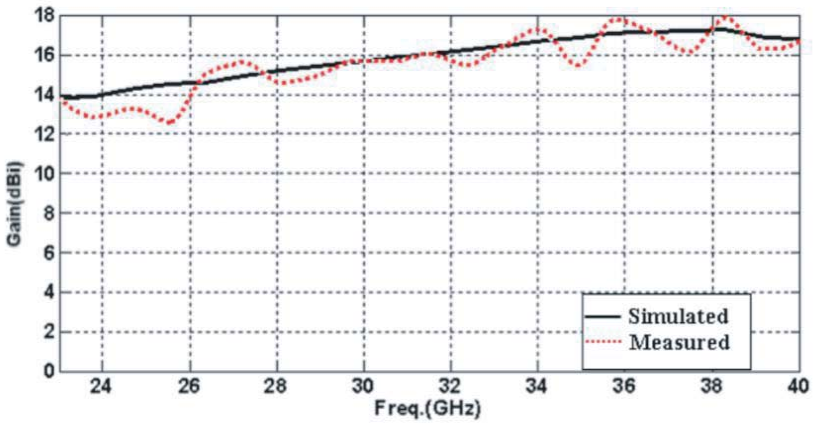

Figure 15. Comparison between the measured and simulated antenna gain of the modified Vivaldi antenna.

the measured and simulated antenna peak gains is presented in Fig. 15. It can be noted that a good agreement between the measured and simulated gains is obtained.

5. CONCLUSION

The present paper introduces the design of an ENZ metamaterial in the mm-wave frequency range from 23 to 40 GHz. This frequency band has a significance in 5G applications, specifically at 28 and 38 GHz. This ENZ metamaterial is used to enhance the radiation characteristics of a Vivaldi antenna operating in the same frequency range. The design of the Vivaldi antenna is discussed in detail. Two configurations for adding ENZ unit cells in the flare of the Vivaldi antenna are studied. These two configurations are based on extending the Vivaldi antenna with a rectangular or a triangular substrate loaded by the ENZ metamaterial. Both configurations show improvements in the matching and antenna gain. However, the second configuration has a better performance. The second configuration shows an improvement in antenna gain around 5 dB in the operating frequency range. This configuration is fabricated and measured experimentally. Good agreements between the simulated and measured results are obtained.

REFERENCES

1. Priyadharisini, S. G. and E. Rufus, "A double negative metamaterial inspired miniaturized rectangular patch antenna with improved gain and bandwidth," *Progress In Electromagnetics Research Symposium — Fall (PIERS — FALL)*, 2907–2913, Singapore, Nov. 19–22, 2017.
2. Ziolkowiski, R. W., "Design, fabrication and testing of double negative metamaterials," *IEEE Transactions on Antennas and Propagation*, Vol. 51, No. 7, 1516–1528, 2003.
3. El-Nady, S., H. Zamel, M. Hendy, A. Attiya, and A. Zekry, "Performance enhancement of end-fire bow-tie antenna by using zero index metamaterial," *Progress In Electromagnetics Research Symposium — Fall (PIERS — FALL)*, 1895–1900, Singapore, Nov. 19–22, 2017.
4. Popescu, A.-S., I. Bendoym, T. Rexhepi, and D. Crouse, "Anisotropic zero index material: A method of reducing the footprint of Vivaldi antennas in the UHF range," *Progress In Electromagnetics Research C*, Vol. 65, 33–43, 2016.
5. Zhou, B. and T. J. Cui, "Directivity enhancement to Vivaldi antennas using compactly anisotropic zero-index metamaterials," *IEEE Antennas and Wireless Propagation Letters*, Vol. 10, 326–329, 2011.
6. Shaw, T., A. Roy, and D. Mitra, "Efficiency enhancement of wireless power transfer system using MNZ metamaterials," *Progress In Electromagnetics Research C*, Vol. 68, 11–19, 2016.

7. Wu, B.-I., W. Wang, J. Pacheco, X. Chen, T. M. Grzegorczyk, and J. A. Kong, "A study of using metamaterials as antenna substrate to enhance gain," *Progress In Electromagnetics Research*, Vol. 51, 295–328, 2005.
8. Alu, A., M. G. Silveirinha, A. Salandrino, and N. Engheta, "Epsilon-near-zero metamaterials and electromagnetic sources: Tailoring the radiation phase pattern," *Physical Review B*, Vol. 75, No. 15, 2007.
9. Silveirinha, M. G. and N. Engheta, "Tunneling of electromagnetic energy through sub-wavelength channels and bends using ε-near-zero materials," *Physical Review Letters*, Vol. 97, No. 15, 2006.
10. Enoch, S., G. Tayeb, P. Sabouroux, N. Guerin, and P. Vincent, "A metamaterial for directive emission," *Physical Review Letters*, Vol. 89, No. 21, 213902, 2002.
11. Wang, B. and K.-M. Huang, "Shaping the radiation pattern with mu and epsilon-near-zero metamaterials," *Progress In Electromagnetics Research*, Vol. 106, 107–119, 2010.
12. Silveirinha, M. G., A. Alù, B. Edwards, and N. Engheta, "Overview of theory and applications of epsilon-near-zero materials," *URSI General Assembly*, 44–47, 2008.
13. Ziolkowski, R. W., "Propagation in and scattering from a matched metamaterial having a zero index of refraction," *Physical Review E*, Vol. 70, No. 4, 2004.
14. Zhou, B., H. Li, X. Zou, and T.-J. Cui, "Broadband and high-gain planar Vivaldi antennas based on inhomogeneous anisotropic zero index metamaterial," *Progress In Electromagnetics Research*, Vol. 120, 235–247, 2011.
15. Pandey, G., H. Singh, and M. Meshram, "Meander-line-based inhomogeneous anisotropic artificial material for gain enhancement of UWB Vivaldi antenna," *Applied Physics A*, Vol. 122, No. 2, 134(1–9), 2016.
16. Nor, N. M., M. H. Jamaluddin, M. R. Kamarudin, and M. Khalily, "Rectangular dielectric resonator antenna array for 28 GHz applications," *Progress In Electromagnetics Research C*, Vol. 63, 53–61, 2016.
17. Parchin, N., M. Shen, and G. Pedersen, "End-Fire phased array 5G antenna design using leaf-shaped bow-tie elements for 28/38 GHz MIMO applications," *IEEE International Conference on Ubiquitous Wireless Broadband*, 2016.
18. Haraz, O., M. Ali, S. Alshebeili, and A. Sebak, "Design of a 28/38 GHz dual-band printed slot antenna for the future 5G mobile communication networks," *IEEE International Antennas Symposium and Propagtion*, 1532–1533, 2015.
19. Hamzah, N. and K. A. Othman, "Designing Vivaldi antenna with various sizes using CST software," *Proceeding of the World Congress on Engineering (WCE 2011)*, 1–5, London, UK, 2011.
20. Wang, Y. W., G. M. Wang, and B. F. Zong, "Directivity improvement of Vivaldi antenna using double-slot structure," *IEEE Antennas and Wireless Propagation Letters*, Vol. 12, 1380–1383, 2013.
21. Molaei, A., M. Kaboli, S. A. Mirtaheri and S. Abrishamian, "Beam-tilting improvement of balanced antipodal vivaldi antenna using a dielectric lens," *Proc. 2nd Iranian Conference on Engineering Electromagnetics*, 577–581, Tehran, Iran, 2014.
22. Fei, P., Y. C. Jiao, W. Hu, and F. S. Zhang, "A miniaturized antipodal Vivaldi antenna with improved radiation characteristics," *IEEE Antennas and Wireless Propagation Letters*, Vol. 10, 127–130, 2011.
23. Li, L., X. Xia, Y. Liu, and T. Yang, "Wideband balanced antipodal Vivaldi antenna with enhanced radiation parameters," *Progress In Electromagnetics Research C*, Vol. 66, 163–171, 2016.
24. Wan, F., J. Chen, and B. Li, "A novel ultra-wideband antipodal Vivaldi antenna with trapezoidal dielectric substrate," *Microwave and Optical Technology Letters*, Vol. 60, No. 2, 449–455, 2018.
25. Sun, M., Z. N. Chen, and X. Qing, "Gain enhancement of 60-GHz antipodal tapered slot antenna using zero-index metamaterial," *IEEE Transactions on Antennas and Propagation*, Vol. 61, No. 4, 1741–1746, 2013.
26. Bhaskar, M., E. Johari, Z. Akhter, and M. J. Akhtar, "Gain enhancement of the Vivaldi antenna with band notch characteristics using zero-index metamaterial," *Microwave and Optical Technology Letters*, Vol. 58, No. 1, 233–238, 2016.

27. Chen, X., T. M. Grzegorczyk., B. I. Wu, J. Pacheco, Jr., and J. A. Kong, "Robust method to retrieve the constitutive effective parameters of metamaterials," *Physical Review E*, Vol. 70, No. 1, 2004.
28. Smith, D., S. Schultz, P. Markos, and C. Soukoulis, "Determination of effective permittivity and permeability of metamaterials from reflection and transmission coefficients," *Physical Review B*, Vol. 65, 1–5, 2002.
29. Teni, G., N. Zhang, J. H. Qiu, and P. Y. Zhang, "Research on a novel miniaturized antipodal Vivaldi antenna with improved radiation," *IEEE Antennas and Wireless Propagation Letters*, Vol. 12, 417–420, 2013.
30. Nassar, I. T. and T. M. Weller, "A novel method for improving antipodal Vivaldi antenna performance," *IEEE Transactions on Antennas and Propagation*, Vol. 63, 3321–3324, 2015.
31. Moosazadeh, M. and S. Kharkovsky, "Development of the antipodal Vivaldi antenna for detection of cracks inside concrete members," *Microwave and Optical Technology Letters*, Vol. 57, No. 7, 1573–1578, 2015.
32. Moosazadeh, M., S. Kharkovsky, and J. T. Case, "Microwave and millimetre wave antipodal Vivaldi antenna with trapezoid-shaped dielectric lens for imaging of construction materials," *IET Microwaves Antennas & Propagation*, Vol. 10, No. 3, 301–309, 2016.
33. Wang, N., M. Fang, J. Qiu, and L. Xiao, "Improved design of balanced antipodal Vivaldi for MMW applications," *Antennas and Propagation & USNC/URSI National Radio Science Meeting, IEEE International Symposium*, 2615–2616, 2017.
34. Wan, F., J. Chen, and B. Li, "A novel ultra-wideband antipodal Vivaldi antenna with trapezoidal dielectric substrate," *Microwave and Optical Technology Letters*, Vol. 60, No. 2, 449–455, 2018.
35. Kerns, D. M., "New method of gain measurement using two identical antennas," *Electronics Letters*, Vol. 6, No. 11, 348–349, 1970.